

Field step size and temperature effects on the character of the magnetostructural transformation in a Gd_5Ge_4 single crystal

Z. W. Ouyang*

Materials and Engineering Physics Program, Ames Laboratory of the US DOE, Iowa State University, Ames, Iowa 50011-3020, USA

V. K. Pecharsky† and K. A. Gschneidner, Jr.

Materials and Engineering Physics Program, Ames Laboratory of the US DOE, Iowa State University, Ames, Iowa 50011-3020, USA and Department of Materials Science and Engineering, Iowa State University, Ames, Iowa 50011-2300, USA

D. L. Schlagel and T. A. Lograsso

Materials and Engineering Physics Program, Ames Laboratory of the US DOE, Iowa State University, Ames, Iowa 50011-3020, USA (Received 29 June 2007; revised manuscript received 28 August 2007; published 10 October 2007)

The critical magnetic fields required to induce the magnetostructural transformation below ~ 30 K in Gd_5Ge_4 are dependent on the size of the magnetic-field step employed during isothermal measurements of magnetization: the smaller the step, the lower the critical field. The influence of the magnetic-field step size on the character of the magnetostructural transition in Gd_5Ge_4 diminishes as temperature increases, nearly disappearing above ~ 30 K. Decreasing the size of the field step also leads to the formation of multiple steps in the magnetization. The steps are reproducible in the same sample at low temperatures (below ~ 9 K) but they become stochastic and irreproducible at high temperatures (above ~ 20 K). The varying dynamics of both the magnetization and demagnetization processes is associated with approaching true equilibrium states and, therefore, reduction of the size of the magnetic-field step at low temperatures plays a role similar to the dominant role of thermal fluctuations at high temperatures. Similar phenomena are expected to occur in other martensiticlike systems, e.g., the manganites.

DOI: [10.1103/PhysRevB.76.134406](https://doi.org/10.1103/PhysRevB.76.134406)

PACS number(s): 75.30.Kz, 75.50.Ee, 76.90.+d

I. INTRODUCTION

Over the past several years, intermetallic compounds with the general chemical formula $\text{Gd}_5\text{Si}_x\text{Ge}_{4-x}$ have received considerable attention due to a wealth of interesting behaviors, such as: strong magnetocaloric,^{1,2} magnetostrictive,³ and magnetoresistive^{4,5} effects; spontaneous generation of voltage;⁶ unusual training,⁷ dynamical⁸ and thermal phenomena;⁹ acoustic emissions;¹⁰ and a novel glasslike kinetically retarded state.¹¹ Most of these phenomena have been observed over a range of compositions when $x \leq \sim 2$, and all of them are related to magnetostructural transitions that can be triggered by varying the magnetic field, temperature, or pressure.^{3,12-14} Among other representatives of this family, considerable attention has been paid to Gd_5Ge_4 ($x = 0$) because of its unusual crystallography and magnetism¹⁵⁻¹⁷ and because of the absence of chemical disorder, which is intrinsic to other members of the $\text{Gd}_5\text{Si}_x\text{Ge}_{4-x}$ family with $0 < x < 4$.^{12,18}

At low temperatures and in the presence of a magnetic field, Gd_5Ge_4 exhibits completely irreversible, partially reversible, or fully reversible first-order phase transition from its apparent antiferromagnetic (AFM) ground state¹⁹ to an induced ferromagnetic (FM) state. Simultaneously with changes in long range magnetism, the crystal lattice of Gd_5Ge_4 is transformed from the Sm_5Ge_4 type (AFM) to the Gd_5Si_4 type (FM), both of which are low-dimensional, layered structures.^{20,21} Varying reversibility reveals a potential for magnetic metastabilities across the AFM-FM transition, which were investigated earlier by magnetic relaxation measurements in polycrystalline Gd_5Ge_4 .²² The relaxation of

magnetization was ascribed to a disorder-influenced first-order phase transition and related superheating or undercooling. The relaxation at 25 K is smaller than that at 5 K, but it was not studied systematically. Furthermore, a kinetically retarded glassy magnetic state may also contribute to the observed time dependencies.¹¹ Magnetic relaxation is found in many magnetic materials, such as a spin-chain compound $\text{Ca}_3\text{Co}_2\text{O}_6$,²³ a compound with quantum tunneling of magnetization $\text{BaFe}_{10.2}\text{Sn}_{0.74}\text{Co}_{0.66}\text{O}_{19}$,²⁴ and martensiticlike $\text{Ce}(\text{Fe}_{0.96}\text{Ru}_{0.04})_2$ (Ref. 25) and $\text{Pr}_{0.65}(\text{Ca}_y\text{Sr}_{1-y})_{0.35}\text{MnO}_3$,²⁶ and it may be used to determine the stability of a magnetic system

Another form of metastable magnetic response—the influence of magnetic-field sweep rate \dot{H} on isothermal $M(H)$ data during the AFM-FM transition—was investigated in a polycrystalline Gd_5Ge_4 at a single temperature point $T = 2$ K.²⁷ Hardy *et al.* found that reducing \dot{H} from 10 to 1 kOe/min delays magnetic instability, thus shifting a sharp, metamagneticlike discontinuity of the magnetization to high-field values, but simultaneously this also decreases the onset of the AFM-FM transition. When \dot{H} is further reduced to 0.1 kOe/min, the metamagnetic discontinuity transforms into a smooth S-shape $M(H)$ curve with deviations from linearity beginning and ending, respectively, in fields much below and above H_{cr} observed when $\dot{H} = 10$ or 1 kOe/min. The \dot{H} dependent $M(H)$ behavior was assumed to be related to the martensitic character of the structural transformation accompanying the AFM-FM transition in Gd_5Ge_4 .²⁷

Unusual magnetic dynamics related to martensitic strain is also expected to be observed in Gd_5Ge_4 single crystals, but because of microstructural differences, single crystals should exhibit features that will be different from polycrystals. Furthermore, Gd_5Ge_4 displays measurable magnetocrystalline anisotropy, which may result in an anisotropic dynamical response. This anisotropy is related both to the low dimensionality of the crystal structure and to a peculiar antiferromagnetic structure of the compound, in which the magnetic moments of Gd atoms are ferromagnetically coupled within the same layer, but the layers are antiferromagnetically coupled along the c axis in low magnetic fields ($H \leq 8.3$ kOe).^{28–30} A fully reversible spin-flop transition is observed when the magnetic field is applied along the c axis.³⁰

Here, we study how varying the magnetic-field step size (which is similar to varying the magnetic-field sweep rate) affects the AFM-FM transition in single crystal Gd_5Ge_4 by using isothermal $M(H)$ measurements between 2 and 30 K. We show that smaller field steps bring the system closer to equilibrium and result in decreasing the critical field required for the onset of the AFM-FM transition. We also report step-like anomalies of the magnetization (“multistep anomalies”) and examine the stability and the reproducibility of the steps.

II. EXPERIMENTAL DETAILS

Three individual Gd_5Ge_4 single crystal specimens with dimensions $0.77 \times 0.91 \times 0.92$ mm³ (sample 1, henceforth called S1), $1.16 \times 1.18 \times 1.22$ mm³ (S2), and $1.22 \times 1.23 \times 1.30$ mm³ (S3) were extracted from a large single crystal grown using the triarc pulling technique.³¹ The details of the preparation, determination of the crystallographic directions, and basic characterization of the samples can be found in Refs. 30 and 31. The isothermal magnetization (M) measurements were performed from 2 to 30 K in a superconducting quantum interference device (SQUID) magnetometer, MPMS-XL, manufactured by Quantum Design, Inc., USA. Before each $M(H)$ and $M(t)$ measurement sequence, the samples were zero field cooled (ZFC) from the paramagnetic state at 300–2 K and then slowly heated to the desired temperature.

The forward magnetic relaxation measurements were carried out by setting the magnetic field to a value at which M reaches 60–70 emu/g, i.e., approximately $\frac{1}{3}$ of the saturation magnetization (~ 200 emu/g) in the standard field-increasing $M(H)$ measurements and then keeping the field constant while measuring M repeatedly for a given length of time. In the H -decreasing measurements, the field was set so that the magnetization is reduced to about 150 emu/g, i.e., $\frac{3}{4}$ of the saturation magnetization, after the sample was magnetized by a 50 kOe magnetic field. The $M(t)$ measurements began immediately after the target field was attained and remained stable for 2 s.

In our experiments, the magnetic field must be constant during every measurement, which is different from Ref. 27, where the magnetization data were recorded in a vibrating sample magnetometer (VSM) while sweeping the magnetic field. Hence, varying the “field sweep” rate was emulated by

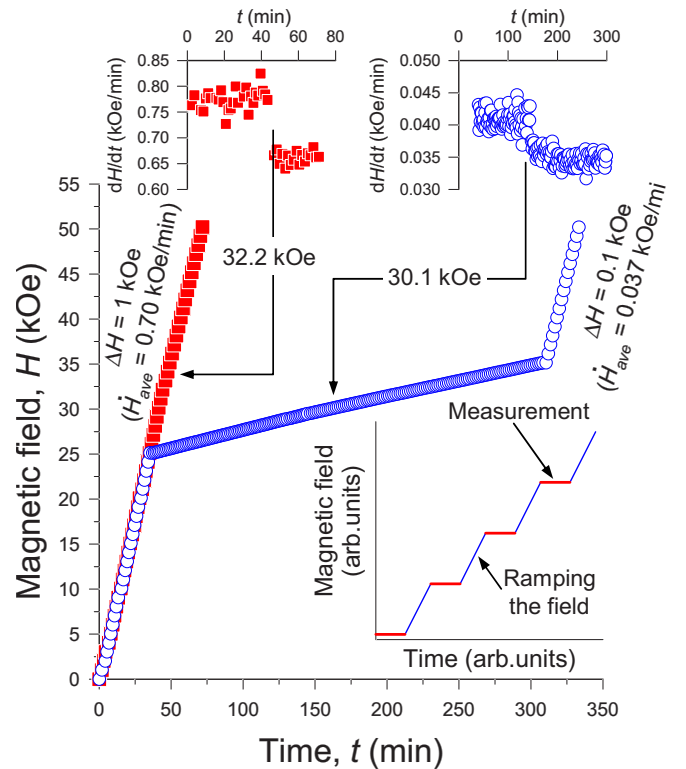


FIG. 1. (Color online) The time dependence of the magnetic field in a SQUID magnetometer when measuring isothermal $M(H)$ data at $T=2$ K with the a axis of the Gd_5Ge_4 single crystal (S1) parallel to the magnetic-field vector. The upper insets show derivatives of $H(t)$ with respect to time visualizing slope changes. The lower inset is a schematic diagram showing that the actual field change includes (1) a pause and a measurement at each fixed field (horizontal lines) and (2) the field increase when charging the magnet (lines with positive slopes).

choosing different sizes of the field increment. Since the behavior of the magnetization in both the AFM and FM states is not affected by the size of the magnetic-field step, a constant field increment $|\Delta H|=1$ kOe was employed for measurements away from the phase transition region, but in the vicinity of the AFM-FM transformations, a range of smaller field step sizes was adopted. Even though the magnetic field does not change linearly with time between two adjacent fixed field measurement points in a SQUID (see the lower inset in Fig. 1), all the fixed field values form nearly a straight line (Fig. 1) except for a small slope change around the critical fields [see the upper insets in Fig. 1 and compare with the critical field values shown in Fig. 2(a)]. For simplicity, we shall assume that the magnetic field changes “linearly” with an average field sweep rate \dot{H}_{av} . For example, $\Delta H=1$ kOe corresponds to $\dot{H}_{av}=0.70$ kOe/min, and $\Delta H=0.1$ kOe to $\dot{H}_{av}\cong 0.037$ kOe/min.

III. EXPERIMENTAL RESULTS

A. Variable field step size and the antiferromagnetic \rightarrow ferromagnetic transition at 2 K

Since the FM \rightarrow AFM transition does not occur in a kinetically retarded state,^{11,32} in this section, we will be con-

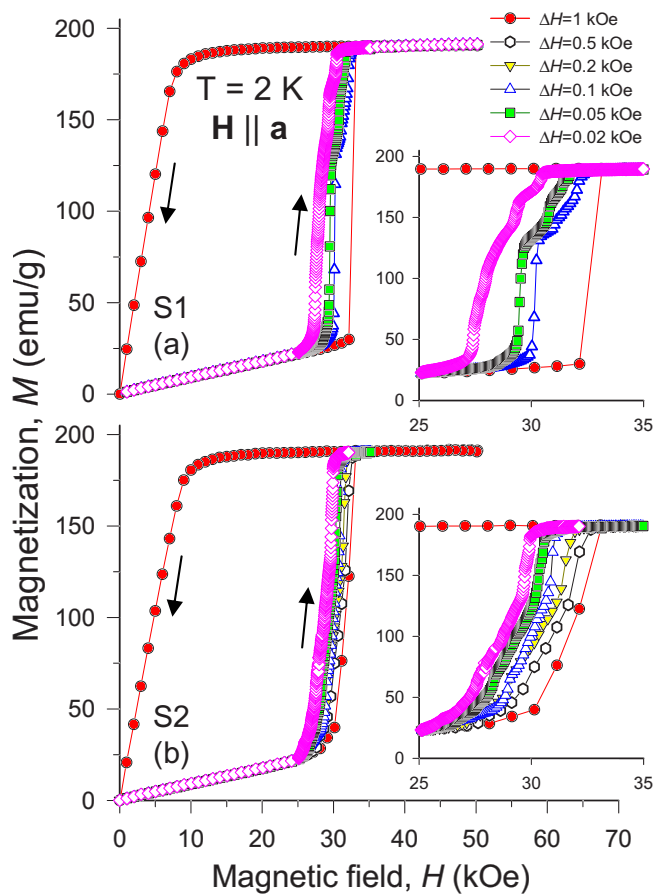


FIG. 2. (Color online) The magnetization isotherms of two different single crystals of Gd_5Ge_4 (S1 and S2) measured at $T=2$ K after zero field cooling from 300 K with the magnetic-field vector parallel to the a axis. The insets clarify details between 25 and 35 kOe, i.e., in the vicinity of the magnetic-field-induced AFM \rightarrow FM transition.

cerned only with applying a magnetic field to a ZFC sample and the resulting field-induced AFM \rightarrow FM transition. Figure 2 shows the $M(H)$ curves of two samples—S1 and S2—with the magnetic-field vector parallel to the a axis. When $\Delta H = 1$ kOe (and greater, not shown), the AFM \rightarrow FM transitions are seen as extremely sharp, nearly discontinuous steps similar to that reported in Ref. 28, especially in S1. When ΔH decreases, a common feature is that the critical fields for both the onset and the completion of the AFM \rightarrow FM transition, H_{c1} and H_{c2} , respectively, shift to lower fields. This behavior is understood by recalling that FM- Gd_5Ge_4 may be slowly induced from the AFM state by undercritical magnetic fields.^{11,16} The same phenomenon (both H_{c1} and H_{c2} are reduced when ΔH decreases) is also observed with the magnetic-field vector parallel to the other two principal crystallographic directions in these two samples. Thus, altering ΔH (or \dot{H}_{av}) in a SQUID magnetometer influences the character of the AFM \rightarrow FM transition, which is similar to the effect of variable \dot{H} in a VSM.

Figure 3 shows the $M(H)$ curves of S3. Similar to S1 and S2, in the measurement with the field increment of $\Delta H = 1$ kOe, the AFM \rightarrow FM transition is very sharp. However,

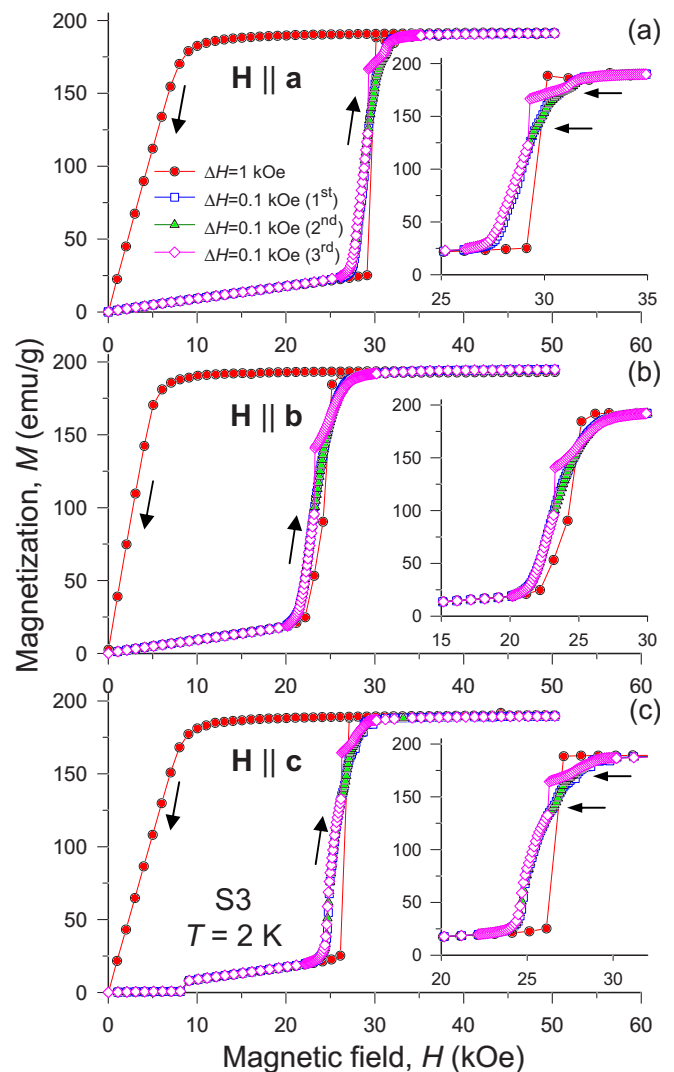


FIG. 3. (Color online) The magnetization isotherms of the ZFC single crystal of Gd_5Ge_4 (S3) measured at $T=2$ K. The field steps with $\Delta H=1$ and 0.1 kOe were employed from 26 to 35 kOe for the a axis, from 20 to 30 kOe for the b axis, and from 22 to 30 kOe for the c axis. These differences were determined by the anisotropy of the magnetic properties of the compound [$H_{c1}(a \text{ axis}) > H_{c1}(c \text{ axis}) > H_{c1}(b \text{ axis})$] (Ref. 30). The first two measurements with $\Delta H=0.1$ kOe were performed without any delays in order to verify reproducibility of the behavior. The third measurements with $\Delta H=0.1$ kOe were interrupted after reaching 29, 23, and 26 kOe for the a , b , and c axes, respectively, and the sample was held in these fields for 50 min before resuming the measurement. The insets clarify the behavior in the immediate vicinity of the field-induced AFM \rightarrow FM transition. The horizontal arrows in the insets in (a) and (c) point to minor magnetization steps.

all $M(H)$ curves measured with $\Delta H=0.1$ kOe exhibit a much smoother AFM \rightarrow FM transition, and thus the transition broadens, occurring over a field range of ~ 7 kOe for all the three axes. The transition starting at a lower field H_{c1} but ending at a higher field H_{c2} when \dot{H}_{av} is reduced is quite different from what is observed in S1 and S2 (see Fig. 2). A substantial difference in the sharpness of the transformation when $\Delta H=1$ kOe, which is truly discontinuous when the

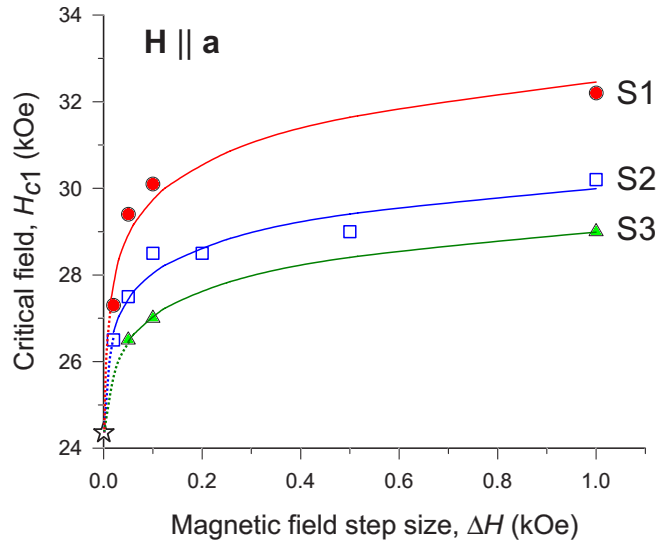


FIG. 4. (Color online) The critical fields H_{c1} (i.e., the onsets of the AFM \rightarrow FM transition) for different samples of Gd_5Ge_4 as functions of the magnetic-field step size measured at $T=2$ K with the magnetic-field vector along the a axis. The solid lines are logarithmic fits of the existing data. The dotted lines represent an estimated common H_{c1} (shown as a star) when ΔH approaches 0.

magnetic field is confined to the ac plane [Figs. 3(a) and 3(c)] but becomes more gradual when the field vector is perpendicular to the ac plane [Fig. 3(b)], is worth noting. This difference in the behavior indicates that higher values of the critical fields lead to sharper transitions compared to the lower critical field leading to a smooth change of M . A similar correlation between the sharpness of the transition and the value of the critical magnetic field is also seen in Fig. 2. These differences may be understood by recalling that at $T=2$ K, the transformation is controlled by the configuration of the devitrification boundary on the phase diagram rather than by the configuration of the AFM \rightarrow FM transition boundary.³² For one crystal (S3, Fig. 3), anisotropic behavior indicates that both the width and the location of the devitrification boundary are anisotropic, while for the other single crystals (S1 and S2, Fig. 2), we conclude that the width of the devitrification boundary is weakly sample dependent.

Taking into account all of the available data, one easily concludes that irrespective of sample differences, the value of H_{c1} is always reduced with the reduction of ΔH or \dot{H} . We believe that this occurs due to the progressively better accommodation of the martensitic strains. As ΔH (or \dot{H}) decreases, the system resides in the fields close to critical longer and, therefore, has enough time for the nucleation and growth of the FM phase even when $H < H_{c1}$ (also see magnetic relaxation data below). The dependencies of H_{c1} on ΔH for three different single crystalline samples are shown in Fig. 4. All H_{c1} vs ΔH curves exhibit a logarithmic variation with the size of field step. Even though the observed critical fields are different from one sample to another, they appear to collapse to the same value $24 < H_{c1} < 25$ kOe as $\Delta H \rightarrow 0$. This behavior indicates that the slower the measurement, the closer the sample is brought to equilibrium. It also suggests that different single crystals have different strain fields due to

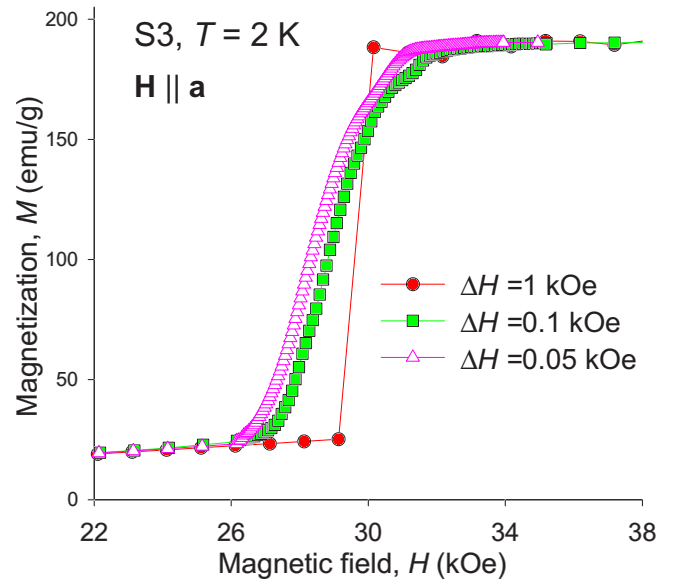


FIG. 5. (Color online) The $M(H)$ isotherms of the ZFC single crystal of Gd_5Ge_4 (S3) measured at 2 K with $\Delta H=1, 0.1,$ and 0.05 kOe between 26 and 35 kOe.

probable variations in mosaicity and other factors related to their microstructure, such as details of their twin structures¹² and concentration of Gd_5Ge_3 platelets.³³

In contrast, the direction toward which the upper critical field, H_{c2} , shifts is not the same, varying from one sample to another. This may be ascribed to irregularities of domain structure and domain wall mobility that will be strongly influenced by any variations of the microstructure of different samples. Similar to H_{c1} , the anomalies in the behavior of H_{c2} are eliminated as ΔH is reduced. This is illustrated in Fig. 5, which indicates that the reduction of ΔH from 0.1 to 0.05 kOe in S3 moves both H_{c1} and H_{c2} to lower field values.

The lower limit of H_{c1} (see Figs. 4 and 5) can also be determined from magnetic relaxation measurements. As an example, the inset of Fig. 6 shows the a -axis $M(t)$ data of S3 measured in several constant fields varying from 10 to 32 kOe. The magnitude of the relaxation, which can be defined as the difference between the magnetization at 2 s and 5 h, is strongly influenced by the proximity of the measurement field to H_{c1} ; the latter is approximately 28 kOe for “conventional” $M(H)$ measurements with $\Delta H=1$ kOe. At and below 24 kOe, the magnetization remains constant over the entire 5 h period. A time-induced metamagnetic transition from the AFM to the FM state is observed in fields between 25.5 and 26.5 kOe. The critical time decreases as the field value approaches H_{c1} : it is about 60 min for $H=26$ kOe, while it is only ~ 20 min for $H=26.5$ kOe. At 27 kOe and higher fields, the FM phase is rapidly induced but the magnetization does not reach saturation even after a 5 h hold until the applied field reaches and exceeds 30 kOe.

The values of magnetization at 2 s and 5 h were extracted and plotted in the main panel of Fig. 6, where the $M(H)$ curves measured with $\Delta H=1$ and 0.05 kOe are also shown for comparison. From these results, the lower limit of H_{c1} is between 24 and 25 kOe, which matches the estimate ob-

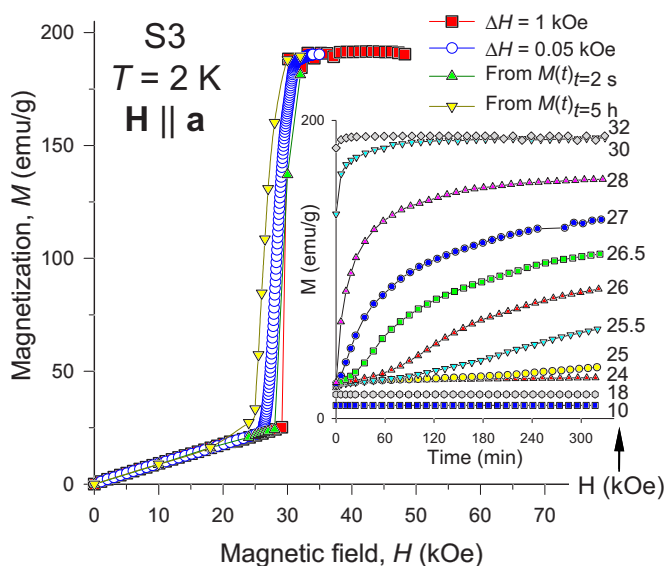


FIG. 6. (Color online) Magnetization vs field measured at $t = 5$ h and $t = 2$ s extracted from the magnetic relaxation measurements at 2 K of the ZFC single crystal of Gd_5Ge_4 (S3). The $M(H)$ curves measured with $\Delta H = 1$ and 0.05 kOe are shown for comparison. The inset shows some of the magnetic relaxation data as $M(t)$ curves. Relaxation measurements were initiated as soon as the specified magnetic field was reached and stable for 2 s.

tained by extrapolating the H_{c1} vs ΔH data to $\Delta H \rightarrow 0$ (see Fig. 4, above) very well. The entire $M(H)$ curve at 5 h is displaced toward lower magnetic-field values with respect to the $M(H)$ curve at 2 s, which serves as an additional confirmation that H_{c2} will also shift toward lower fields when the field increment will become sufficiently small to reach equilibrium.

B. Field-induced multiple steps of magnetization across the antiferromagnetic \rightarrow ferromagnetic transition

In addition to the shifting of H_{c1} and H_{c2} , decreasing ΔH also leads to the appearance of numerous field-induced magnetization steps (multisteps), see Fig. 2. Generally, the lower the ΔH , the clearer the multisteps. The shapes of the magnetization isotherms in the transition region, including the multisteps, are similar in the same sample regardless of ΔH , indicating stability of the multisteps. Yet, their appearance is different from one sample to another (see inset in Fig. 2). Even for S3, where the AFM \rightarrow FM transition is broadened while decreasing ΔH , several small steps are seen clearly for the a and c axes, as shown by horizontal arrows in the Fig. 3 insets. The stability of these small steps was verified by two independent measurements repeated with $\Delta H = 0.1$ kOe, in which both $M(H)$ curves nearly overlap.

Hardy *et al.*^{27,34,35} and Mahendiran *et al.*³⁶ investigated the field spacing effects on the magnetostructural AFM-FM transitions in manganites. A staircaselike $M(H)$ shape was observed in $\text{Pr}_{0.5}\text{Ca}_{0.5}\text{Mn}_{0.95}\text{Ga}_{0.05}\text{O}_3$ in the vicinity of the field-induced magnetic phase transition.³⁴ This behavior was associated with the competition between the magnetic energy promoting the development of the FM phase and elastic en-

ergy associated with the strains near the AFM-FM domain wall interfaces, which tends to block the AFM-FM transition. Noting the staircase likeness of the steps and recalling that the manganites and Gd_5Ge_4 are phase separated systems, in which the AFM and FM phases having different crystal structures coexist, we conclude that microstructural features of each individual specimen play an important role in the formation of the multistep avalanches of M . For a large field step, Gd_5Ge_4 quickly responds to the excess magnetic energy. It has no time to slowly nucleate and grow a new FM phase with the Gd_5Si_4 -type structure in the AFM matrix that maintains the Sm_5Ge_4 -type structure. Yet, as soon as the driving force—the magnetic energy—exceeds a certain threshold, the material overcomes a large, systemwide elastic energy barrier. Thus, a single discontinuity of the magnetization indicating a rapid, burstlike formation of the high magnetic-field phase is observed. For a small field step, the system becomes sensitive to local, smaller energy barriers related to elastic strains at the individual AFM-FM domain wall interfaces. In the vicinity of each local energy barrier, there is ample time to nucleate and grow the FM phase and relieve local stress, thus producing a slow, staircase steplike transition pathway.

On the other hand, the steplike features in the Gd_5Ge_4 single crystal call for a consideration of how the magnetic field varies in a SQUID magnetometer and what effect this may have on the phase transition. When $\Delta H < 1$ kOe, the AFM-FM transition contains multiple, closely spaced fixed field points across the transition. During the pause and the measurement at each point, the FM phase may and likely does continue to either or both nucleate and grow, although the field remains stable (see inset in Fig. 6). Even a relatively slow measurement in a SQUID, therefore, represents a snapshot of a system that may not have come to an equilibrium state for a given combination of temperature and magnetic field. Figure 3 reveals that in the third measurement with $\Delta H = 0.1$ kOe, the $M(H)$ curve initially follows the first and second $M(H)$ curves until the field was held constant for 50 min at 29, 23, and 26 kOe for the a , b , and c axes, respectively. When the field increment was resumed, large magnetization steps appear along each of the three axes. Continuing the measurement with $\Delta H = 0.1$ kOe shows that the magnetization curves are slowly returning to their original magnetization paths and, eventually, all three sets of $M(H)$ data coincide with one another before the AFM \rightarrow FM transition is complete. This behavior indicates that some (but not all) of the observed magnetization multisteps may be extrinsic and, therefore, irreproducible, originating from uneven times the system resides in a constant magnetic field during each measurement, which is in good agreement with the conclusions of Ref. 26.

C. Temperature vs field step size effects

We now consider how temperature changes the sensitivity of the magnetostructural transition in Gd_5Ge_4 to the variable size of the magnetic-field increment. This was done using S2, in which both H_{c1} and H_{c2} shift to lower fields and magnetization multisteps appear at 2 K when the field step size is

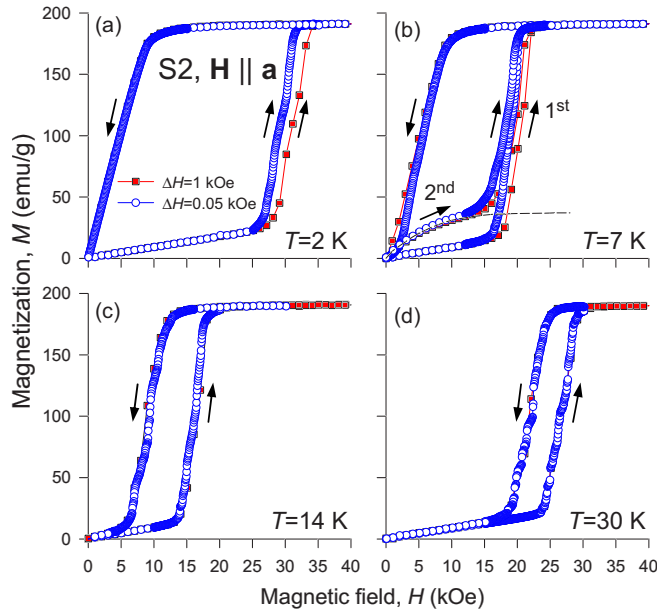


FIG. 7. (Color online) The isothermal magnetization measured at 2, 7, 14, and 30 K with $\Delta H=1$ and 0.05 kOe using single crystal of Gd_5Ge_4 (S2). In all cases except for the second measurement in (b), the sample was zero field cooled from 300 to 2 K and then warmed to the temperature of measurement. The second measurement in (b) was performed isothermally immediately following the first magnetization and demagnetization of the specimen. The arrows show the direction of the magnetic-field change.

reduced to 0.2 kOe and below, as seen in Fig. 2. Figure 7 shows $M(H)$ behaviors of S2 measured at $T=2, 7, 14,$ and 30 K with the magnetic-field vector parallel to the a axis employing two different field steps— $\Delta H=1$ and 0.05 kOe—across the AFM \leftrightarrow FM transition. At 2 K, the H -increasing $M(H)$ exhibits a pronounced shift toward lower field when ΔH is reduced from 1 to 0.05 kOe, as was discussed above. As temperature rises, this effect becomes smaller and the shift of H_{c1} (and H_{c2}) disappears at 30 K. In a second isothermal application of the field, additional broad ferromagnetic steps are observed between 4 and 14 K [see the $T=7$ K isotherm, Fig. 7(b)]. These steps reflect the residual FM phase remaining in the sample after the first magnetization-demagnetization cycle due to kinetic retardation and resulting incomplete reversibility of the transformation.^{11,30,32} The second magnetization curves also reveal shifting of H_{c1} during the transition when ΔH is reduced to 0.05 kOe.

In the field-decreasing measurements, changing the magnetic-field increment also affects the lower critical fields of the FM \rightarrow AFM transition, but somewhat different features are seen when compared to the field-increasing measurements. Thus, $M(H)$ curves measured at $T=2$ K with $\Delta H=1$ and 0.05 kOe shown in Fig. 7(a) nearly fully overlap with one another because the FM \rightarrow AFM transition is fully arrested and the compound remains 100% ferromagnetic. With increasing temperature, the $M(H)$ curves measured with smaller ΔH exhibit a shift toward higher fields compared to the $M(H)$ curves measured with $\Delta H=1$ kOe; this shift is quite substantial at 7 K [Fig. 7(b)]. Above $T=7$ K, the effect

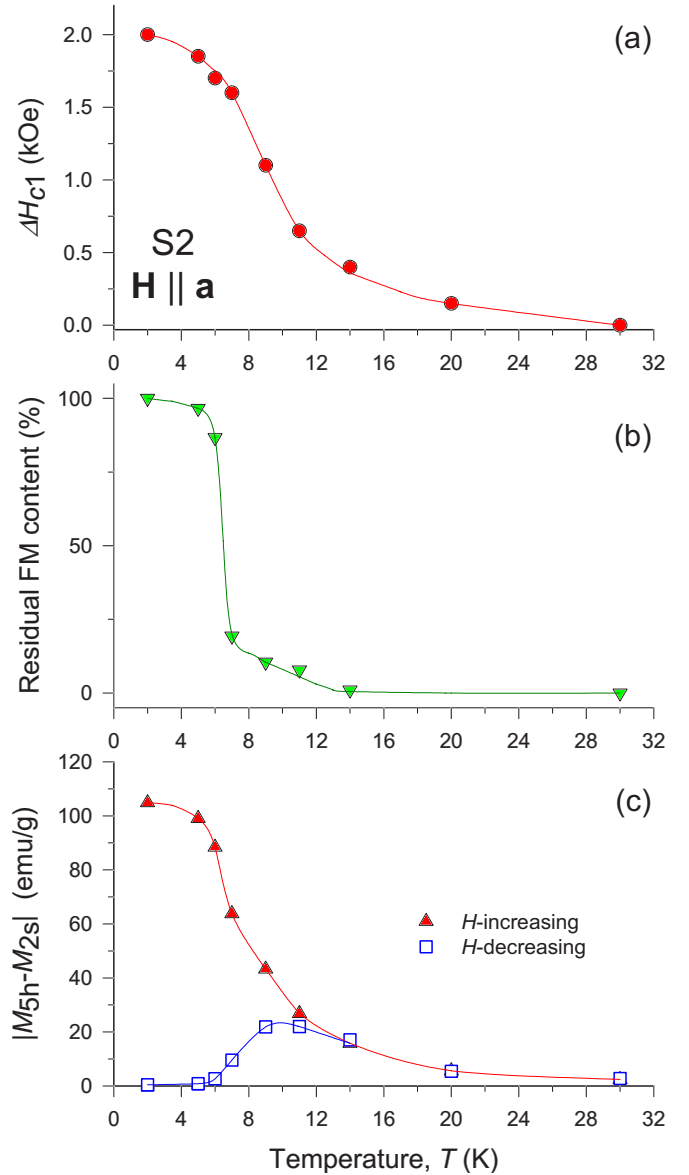


FIG. 8. (Color online) (a) The effect of temperature on the shifting of the critical field, $\Delta H_{c1} = H_{c1, \Delta H=1 \text{ kOe}} - H_{c1, \Delta H=0.05 \text{ kOe}}$ for the ZFC single crystal of Gd_5Ge_4 (S2). (b) The temperature dependence of the residual content of the ferromagnetic phase after the field has been removed. (c) The temperature dependence of the magnitude of the magnetic relaxation in the H -increasing and H -decreasing $M(H)$ curves of S2.

becomes smaller [Fig. 7(c)] and both $M(H)$ curves measured with $\Delta H=1$ and 0.05 kOe overlap with one another at and above ~ 30 K [Fig. 7(d)]. We note that effects of varying field step were similar for the b and c axes, but these data are not shown here.

The effect of variable magnetic-field increment size on the phase transition in Gd_5Ge_4 can be quantified by analyzing the difference between H_{c1} observed with different ΔH , which for the two field step sizes chosen here is defined as $\Delta H_{c1} = H_{c1, \Delta H=1 \text{ kOe}} - H_{c1, \Delta H=0.05 \text{ kOe}}$. The temperature dependence of ΔH_{c1} for the ZFC $M(H)$ curves is shown in Fig. 8(a), indicating that at 30 K and above, varying ΔH (or varying field sweep rate) no longer affects the character of the

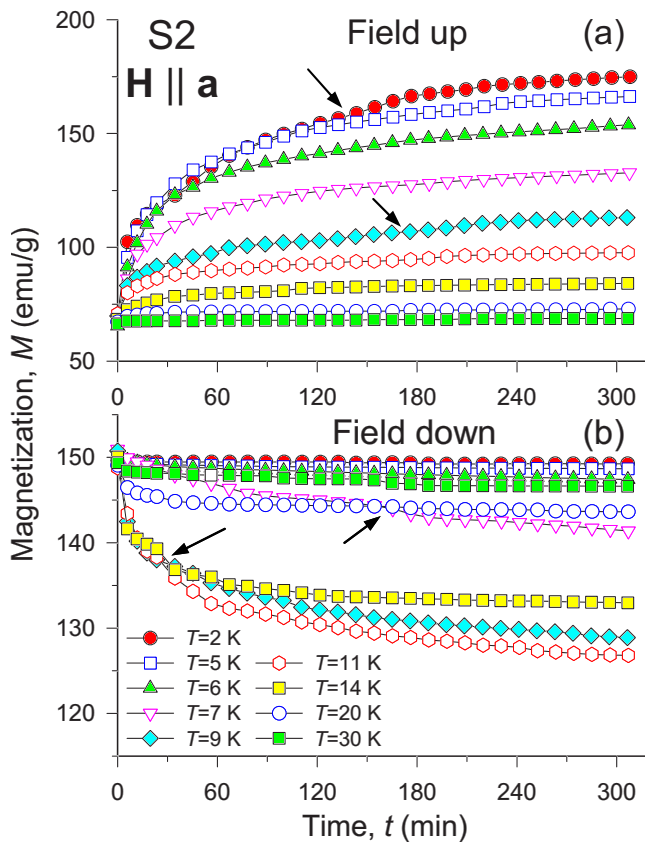


FIG. 9. (Color online) Time evolution of the magnetization of single crystal of Gd_5Ge_4 (S2) with a fixed magnetic field between H_{c1} and H_{c2} applied along the a axis of the crystal. Field at each temperature was chosen to reach $\sim 33\%$ (~ 66 emu/g) of the saturation moment in the H -increasing $M(H)$ curves and $\sim 75\%$ (~ 150 emu/g) in the H -decreasing data. The arrows point to some of the observed magnetization steps.

magnetostructural transition. Figure 8(b) shows the content of the residual FM phase after the ZFC single crystal has been magnetized and demagnetized once, determined from low-field $M(H)$ data using relatively large magnetic-field increments of $\Delta H = 1$ kOe. This plot reflects the extent of kinetic retardation in this particular specimen, indicating that it is completely suppressed in this single crystal at 14 K and higher temperatures. Considering both the similarities and differences of the behavior shown in Figs. 8(a) and 8(b), it appears that although the formation of a glassy state at low temperatures plays a major role in determining magnetic metastabilities in the Gd_5Ge_4 crystals, there may be other factors that are responsible for the time dependent behavior of the magnetization above ~ 14 K.

The weakening of the field step size effect suggests that the magnetic relaxation across the magnetostructural transformation is suppressed with the increasing temperature. Figure 9 shows the results of the magnetic relaxation measurements performed with the magnetic-field vector parallel to the a axis at different temperatures during both the magnetization and demagnetization of S2. In the H -increasing data [Figs. 9(a) and 8(c)], the magnitude of the relaxation defined as $|M_{5h} - M_{2s}|$ is quite large at 2 K. With increasing temperature, the relaxation gradually weakens, practically disap-

pearing at 30 K. The temperature dependence of $|M_{5h} - M_{2s}|$ exhibits behavior similar to the temperature dependence of ΔH_{c1} [see Figs. 8(c) and 8(a)]. However, in the H -decreasing $M(H)$ curves [Figs. 9(b) and 8(c)], the system shows the strongest relaxation around 10 K, on both sides of which the relaxation is rapidly reduced.

Generally, magnetic relaxation phenomena are a direct consequence of metastable magnetic states, indicating that a system relaxes toward its stable magnetic state. Metastable states, which are separated by some energy barriers, are known to exist in a wide variety of magnetic materials.^{23–26} With the barriers due to elastic strain being the highest near domain wall interfaces across the AFM-FM transition in a single crystal of Gd_5Ge_4 , it is reasonable to assume that the competition between strain, magnetic, and thermal activation energies is responsible for changing the dynamics of the magnetic response across the magnetostructural transition in this system. At 2 K, thermal fluctuations are weak and, therefore, magnetic energy must be dominant in overcoming strain energy barriers. Thus, when the magnetic field is near H_{c1} , especially when a smaller field step size is employed, nucleation and growth of the FM phase in the AFM matrix occur near the lowest strain energy barriers, the distribution of which in the bulk is established by microstructural peculiarities of each individual specimen. This results in a strong magnetic relaxation in the H -increasing curves because the formation and growth of FM nuclei alter the strain energy landscape in the crystal, decreasing some barriers, while increasing others. Accordingly, H_{c1} and the whole AFM-FM process shifts to lower field values when ΔH is reduced. Once the metastable AFM matrix is transformed into a stable FM state at 2 K, a different strain energy landscape is formed, and removal of the magnetic field is no longer capable to initiate ($T = 2$ K) or complete ($2 \text{ K} < T < 14$ K) the reverse FM \rightarrow AFM transition, resulting in a kinetic arrest.

As temperature rises, the thermal energy rapidly increases, and thermal fluctuations become dominant in overcoming the strain energy barriers. This follows from the reduction of the width of the hysteresis in the $M(H)$ curves when temperature changes from 2 to 30 K (see Fig. 7). Above ~ 30 K, thermal fluctuations control the nucleation and growth of the FM phase in the AFM matrix at each given combination of H and T , quickly leading to an equilibrium state regardless of the size of ΔH , thus minimizing magnetic relaxation and eliminating the field step size dependent character of the AFM \rightarrow FM transition.

Signatures of thermal activation are also seen in the $\Delta H = 0.05$ kOe $M(H)$ curves at 14 and 30 K (see Fig. 7), where numerous discontinuous magnetization steps are obvious. Repeated measurements at 30 K reveal that while the magnetization discontinuities between the AFM and FM states are reproducible, the smaller, local steps occurring in the phase separated state (i.e., those observed along the sharp rises and drops of the magnetization) are stochastic and irreproducible (actual data are not shown here for conciseness), which is quite different from the reproducible magnetization multisteps observed at 2 K (see Sec. III B above).

The magnetic relaxation curves shown in Fig. 9 also exhibit several steps, some of which are shown by arrows in the

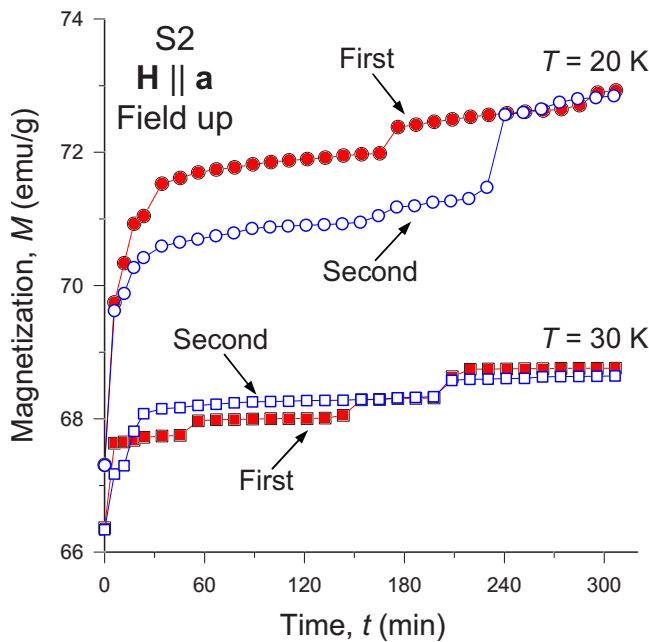


FIG. 10. (Color online) Time evolution of the magnetization of the ZFC single crystal of Gd_5Ge_4 (S2) measured at 20 and 30 K repeatedly at the same fixed field located between H_{c1} and H_{c2} with the magnetic-field vector parallel to the a axis of the crystal.

figure. The steps observed from 2 to 9 K are smooth but those appearing above 14 K become sharper. Close examination of the $M(t)$ behavior reveals that the relaxation data at 20 and 30 K exhibit several discontinuous steps with the magnetization changing very slowly before and after each of the steps, which is shown in Fig. 10. Irreproducibility once again indicates that these steps are stochastic (thermally activated), and therefore they are similar in origin to the discontinuous steps observed in the 14 and 30 K $M(H)$ curves (see Fig. 7). Similar steps were also observed in polycrystals.²²

Based on the evidence shown above, the metastable AFM matrix can be rapidly converted into the equilibrium FM state when thermal fluctuations easily overcome local energy barriers, which is similar to approaching the equilibrium FM state over longer periods of time when the field step size is reduced in the $M(H)$ measurements. This suggests that the

critical fields H_c for the AFM-FM transition in Gd_5Ge_4 determined previously from nonequilibrium $M(H)$ measurements (usually with ΔH at or greater than 1 kOe^{15,16,28,30,37}) are not true critical fields. Thus, the temperature ranges where the irreversible and reversible AFM-FM transitions coexist, i.e., from 10 to 20 K for polycrystals^{16,37} and from 4 to 14 K for single crystals,³⁰ respectively, are only true for these relatively quick, nonequilibrium magnetization measurements. From Fig. 8(c), which reflects the closest to the equilibrium state, the temperature range where both irreversible and reversible AFM-FM transition coexist may be estimated to be from 4 to 30 K in single crystal Gd_5Ge_4 . Above 14 K, the magnetic relaxation is weak, indicating that only small volumes of the specimen's bulk remain kinetically arrested, and the residual FM content is difficult if not impossible to detect by nonequilibrium $M(H)$ measurements.

IV. CONCLUSIONS

The character of the AFM-FM transition in a single crystal of Gd_5Ge_4 is greatly affected by the size of the magnetic-field step or the average field change rate, \dot{H}_{av} . The reduction of field step shifts both the beginning and the end of the AFM-FM transition to lower field values regardless of the geometrical relationship between the magnetic-field vector and any of the three principal crystallographic directions. The smaller the field steps and the slower the measurements, the closer the system is to the equilibrium state. Small but frequent discontinuities of the magnetization, i.e., the magnetization multisteps, that occur during the transition are different for different samples, but they are reproducible for a single sample. With increasing temperature, the effects of varying field step size are weakened and disappear above ~ 30 K. The change of the dynamic magnetic response with temperature can be understood by considering the competition between magnetic, strain, and thermal energies.

ACKNOWLEDGMENTS

The Ames Laboratory is operated for the U.S. Department of Energy by Iowa State University of Science and Technology. This work was supported by the Department of Energy, Office of Basic Energy Sciences, Materials Sciences Division under Contract No. DE-AC02-07CH11358.

*Present address: Institute for Materials Research, Tohoku University, 2-1-1 Katahira, Aoba-ku, Sendai 980-8577, Japan.

†Corresponding author; vitkp@ameslab.gov

¹V. K. Pecharsky and K. A. Gschneidner, Jr., *Phys. Rev. Lett.* **78**, 4494 (1997).

²V. K. Pecharsky and K. A. Gschneidner, Jr., *Appl. Phys. Lett.* **70**, 3299 (1997).

³L. Morellon, P. A. Algarabel, M. R. Ibarra, J. Blasco, B. García-Landa, Z. Arnold, and F. Albertini, *Phys. Rev. B* **58**, R14721 (1998).

⁴L. Morellon, J. Stankiewicz, B. García-Landa, P. A. Algarabel, and M. R. Ibarra, *Appl. Phys. Lett.* **73**, 3462 (1998).

⁵E. M. Levin, V. K. Pecharsky, and K. A. Gschneidner, Jr., *Phys. Rev. B* **60**, 7993 (1999).

⁶E. M. Levin, V. K. Pecharsky, and K. A. Gschneidner, Jr., *Phys. Rev. B* **63**, 174110 (2001).

⁷M. Manekar, M. K. Chattopadhyay, R. Kaul, V. K. Pecharsky, and K. A. Gschneidner, Jr., *J. Phys.: Condens. Matter* **18**, 6017 (2006).

⁸F. Casanova, A. Labarta, X. Batlle, E. Vives, J. Marcos, L. Mañosa, and A. Planes, *Eur. Phys. J. B* **40**, 427 (2004).

⁹F. Casanova, A. Labarta, X. Batlle, F. J. Pérez-Reche, E. Vives, L. Mañosa, and A. Planes, *Appl. Phys. Lett.* **86**, 262504 (2005).

¹⁰F. J. Pérez-Reche, F. Casanova, E. Vives, L. Mañosa, A. Planes, J.

- Marcos, X. Batlle, and A. Labarta, Phys. Rev. B **73**, 014110 (2006).
- ¹¹S. B. Roy, M. K. Chattopadhyay, P. Chaddah, J. D. Moore, G. K. Perkins, L. F. Cohen, K. A. Gschneidner, Jr., and V. K. Pecharsky, Phys. Rev. B **74**, 012403 (2006).
- ¹²W. Choe, V. K. Pecharsky, A. O. Pecharsky, K. A. Gschneidner, Jr., V. G. Young, Jr., and G. J. Miller, Phys. Rev. Lett. **84**, 4617 (2000).
- ¹³L. Morellon, J. Blasco, P. A. Algarabel, and M. R. Ibarra, Phys. Rev. B **62**, 1022 (2000).
- ¹⁴C. Magen, Z. Arnold, L. Morellon, Y. Skorokhod, P. A. Algarabel, M. R. Ibarra, and J. Kamarad, Phys. Rev. Lett. **91**, 207202 (2003).
- ¹⁵E. M. Levin, V. K. Pecharsky, K. A. Gschneidner, Jr., and G. J. Miller, Phys. Rev. B **64**, 235103 (2001).
- ¹⁶E. M. Levin, K. A. Gschneidner, Jr., and V. K. Pecharsky, Phys. Rev. B **65**, 214427 (2002).
- ¹⁷F. Casanova, A. Labarta, X. Batlle, J. Marcos, L. Mañosa, A. Planes, and S. de Brion, Phys. Rev. B **69**, 104416 (2004).
- ¹⁸S. Misra and G. J. Miller, J. Solid State Chem. **179**, 2290 (2006).
- ¹⁹D. Paudyal, V. K. Pecharsky, K. A. Gschneidner, Jr., and B. N. Harmon, Phys. Rev. B **75**, 094427 (2007).
- ²⁰V. K. Pecharsky, A. P. Holm, K. A. Gschneidner, Jr., and R. Rink, Phys. Rev. Lett. **91**, 197204 (2003).
- ²¹Ya. Mudryk, A. P. Holm, K. A. Gschneidner, Jr., and V. K. Pecharsky, Phys. Rev. B **72**, 064442 (2005).
- ²²M. K. Chattopadhyay *et al.*, Phys. Rev. B **70**, 214421 (2004).
- ²³V. Hardy, M. R. Lees, O. A. Petrenko, D. M. Paul, D. Flahaut, S. Hébert, and A. Maignan, Phys. Rev. B **70**, 064424 (2004).
- ²⁴X. X. Zhang, J. M. Hernández, J. Tejada, R. Sole, and X. Ruiz, Phys. Rev. B **53**, 3336 (1996).
- ²⁵M. K. Chattopadhyay, S. B. Roy, A. K. Nigam, K. J. S. Sokhey, and P. Chaddah, Phys. Rev. B **68**, 174404 (2003).
- ²⁶T. Wu and J. F. Mitchell, Phys. Rev. B **69**, 100405(R) (2004).
- ²⁷V. Hardy *et al.*, Phys. Rev. B **69**, 020407(R) (2004).
- ²⁸E. M. Levin, K. A. Gschneidner, Jr., T. A. Lograsso, D. L. Schlagegel, and V. K. Pecharsky, Phys. Rev. B **69**, 144428 (2004).
- ²⁹L. Tan *et al.*, Phys. Rev. B **71**, 214408 (2005).
- ³⁰Z. W. Ouyang, V. K. Pecharsky, K. A. Gschneidner, Jr., D. L. Schlagegel, and T. A. Lograsso, Phys. Rev. B **74**, 024401 (2006).
- ³¹D. L. Schlagegel, T. A. Lograsso, A. O. Pecharsky, and J. A. Sampaio, in *Light Metals 2005*, edited by H. Kvande (The Minerals, Metals and Materials Society, TMS, Warrendale, PA, 2005), p. 1177.
- ³²S. B. Roy, M. K. Chattopadhyay, A. Bannerjee, P. Chaddah, J. D. Moore, G. K. Perkins, L. F. Cohen, K. A. Gschneidner, Jr., and V. K. Pecharsky, Phys. Rev. B **75**, 184410 (2007).
- ³³O. Ugurlu, L. S. Chumbley, D. L. Schlagegel, and T. A. Lograsso, Acta Mater. **54**, 1211 (2006).
- ³⁴V. Hardy, S. Hébert, A. Maignan, C. Martin, M. Hervieu, and B. Raveau, J. Magn. Magn. Mater. **264**, 183 (2003).
- ³⁵V. Hardy, S. Majumdar, M. R. Lees, D. McK. Paul, C. Yaicle, and M. Hervieu, Phys. Rev. B **70**, 104423 (2004).
- ³⁶R. Mahendiran, A. Maignan, S. Hébert, C. Martin, M. Hervieu, B. Raveau, J. F. Mitchell, and P. Schiffer, Phys. Rev. Lett. **89**, 286602 (2002).
- ³⁷H. Tang, V. K. Pecharsky, K. A. Gschneidner, Jr., and A. O. Pecharsky, Phys. Rev. B **69**, 064410 (2004).